E-ISSN: 2664-6773
P-ISSN: 2664-6765
Impact Factor: RJIF 5.72
IJCBS 2025; 7(2): 119-133
www.chemicaljournal.org
Received: 21-06-2025
Accepted: 24-07-2025

Diaa M Najim
Directorate of Education, Kirkuk, Ministry of Education, Kirkuk, Iraq

Mohammad M Al-Tufah
Directorate of Education, Kirkuk, Ministry of Education, Kirkuk, Iraq

Anaam Khalif Al-Azzawy
Salah Al-Din Education Directorate, Iraq

Corresponding Author:
Diaa M Najim
Directorate of Education, Kirkuk, Ministry of Education, Kirkuk, Iraq

Synthesis, Spectroscopic Analysis, of Biological and Molecular Docking Assessment of Azo Dye Derivative and Novel Schiff Bases of Cefdinir

Diaa M Najim, Mohammad M Al-Tufah and Anaam Khalif Al-Azzawy

DOI: https://www.doi.org/10.33545/26646765.2025.v7.i2b.162

Abstract
In this study, new compounds of cfedinir were prepared. The dye An1 was prepared in two steps: in the first step, the diazonium salt of cfedinir was prepared by reacting it with sodium nitrite in the presence of concentrated hydrochloric acid. In the second step, the resulting diazonium salt was coupled with 4-chlorobenzaldehyde. Schiff base derivatives of cfedinir were also prepared by reacting cefedrine with benzaldehyde and acetophenone substitutes an acidic medium using ethanol as a solvent. The prepared compounds were characterized by measuring their melting points and by using spectroscopic methods: infrared spectroscopy (FT-IR), proton nuclear magnetic resonance spectroscopy (1H-NMR), and carbon nuclear magnetic resonance spectroscopy (13C-NMR). The structure of the prepared compounds was also confirmed using mass spectra. The mass spectra of the compounds An1 and An2 were measured, and the correctness of the preparation of these compounds was confirmed by matching the calculated molecular mass of these compounds with the measured molar mass. The biological activity of compounds An1, An4, and An2 against two types of Gram-positive (Enterococcus faecalis and Staphylococcus aureus), and Gram-negative (Klebsiella, Pseudomonas) bacteria was evaluated using the agar well diffusion method. It was found that these compounds were highly effective against these types of bacteria, especially at high concentrations. Compound An1 showed inhibition zones of 36 mm and 22 mm against inhibition zones of 18 mm against Klebsiella, and compound An4 showed inhibition zones of 16 mm against Pseudomonas at high concentrations. An1 and An4 were molecularly docked with estrogen receptor alpha (PDB ID: 5T92) and demonstrated stable binding, with binding affinities of -8.43 Kcal/mol for An1 and -8.03 Kcal/mol for An4, in comparison to the standard compound at -7.92 Kcal/mol. Hydrogen bonds and hydrophobic interactions supported this binding. Finally, the structures of compounds An1, An2, and An4 were analyzed using a scanning electron microscope. This study confirms that the production of new compounds with multiple targets can be achieved through structural tuning of these compounds and that future research could improve the effectiveness of these compounds *in vivo*.

Keywords: Cefdinir, Schiff bases, azo dyes, biological activity, and Molecular docking.

Introduction
Cefdinir belongs to the fourth group of biopharmaceuticals, which includes third-generation cephalosporins. Cefdinir has limited solubility and permeability, which may restrict its oral bioavailability [1, 2]. Several sensitive bacterial illnesses, including community-acquired pneumonia, can be treated with cefdinir, a broad-spectrum antibiotic that has strong antibacterial action against both gram-positive and gram-negative bacteria [3, 4]. Its chemical composition is characterized by containing (Z) -2-(2-amino-4-thiazolyl)-2-(hydroxyimino) acetyl moiety at C-7 and vinyl group at C-3 [5]. A broad-spectrum, three-generation oral cephalosporin used to treat respiratory tract infections, including pneumonia, sinusitis, and bronchitis [6]. Cefdinir's (CED) structure is illustrated in (Figure 1) [7]. Additionally, bronchitis is treated with it. Because of its brief half-life of 1.7 hours in humans, regular dosage is necessary to guarantee effectiveness and maintain appropriate systemic exposure of therapy. It's not very soluble either. In addition, it is inexpensive and has little adverse effects [8]. Cefdinir exhibits limited solubility at an acidic pH of less than 4.0, making it a weakly acidic medication. When a medicine is taken orally, pH-related dissolution causes a reduction in the rate of dissolution, which impairs absorption and bioavailability [9]. Schiff bases are often known as the azomethine group in organic chemistry. This group is represented by the formula RHC=N-R1, where the corresponding R or R1 in Schiff bases can be an alkyl, heterocyclic, or aryl group [10]. Schiff bases are created when a primary amine reacts with

carbonyl (aldehydes or ketones) under certain circumstances [11]. The pharmacological and biological activity of schiff bases, particularly those associated with heterocyclic moiety, included antifungal [12], antibacterial [13], antimalarial [14], antioxidant [15], cytotoxic effects [16], anti-inflammatory [17], and anticonvulsant [18]. One of the most significant colored organic compounds are azo compounds, which are distinguished by the presence of the group (-N=N-) in their composition. They are versatile because they inhibit the formation of proteins and RNAs. They also have medicinal applications because they have antibacterial and anti-cancer properties. They are also regarded as one of the key intermediates in the synthesis of numerous other organic compounds and have numerous applications in the field of inorganic chemistry because they are crucial ligands in the formation of numerous coordination complexes [19]. Conjugation and condensation are the chemical reactions used in this work to create new compounds by combining the cefdinir molecule with azo groups and Schiff bases, respectively. As a result, new compounds are created that incorporate the distinct qualities of every functional group. Cefdinir's pharmacological characteristics, such as its ability to combat certain resistant bacterial strains, may be enhanced via chemical modification.

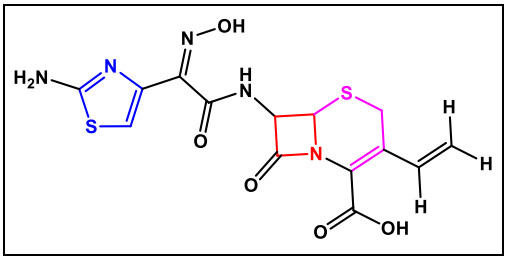

Fig 1: structure of Cefdinir

Materials and Methods

All compounds mentioned in this research were purchased from their manufacturers such as Fluka, Aldrich, BDH and used without any further purification. A thermoelectric device to monitor melting points and a Shimadzu FT-spectrophotometer to capture FT-IR spectra were among the instruments utilized in this study to measure the outcomes. With KBr operating at 400 MHz and DMSO serving as the solvent, 1H-N.M.R. and 13C-N.M.R. spectra were captured using a magnetic spectrometer. A mass spectrometer was used to record the mass spectra. The compounds were characterized by electron microscopy investigation using a Scanning Electron Microscope (SEM) and molecular docking investigations utilizing Molecular Operating Environment (MOE) software (2015).

Synthesis of dye (An1)

A) Diazotization of Amine. [20]

To prepare the solution, Cefdinir 1.97 g (0.005 mol) was dissolved in 5 mL of concentrated HCl. The resulting mixture was then cooled to 0-5 °C in an ice bath. An aqueous solution of $NaNO_2$ 0.33 g (0.005 mol) in 10 mL of water was subsequently added dropwise to the cold Cefdinir solution over a period of 15-20 minutes, while maintaining the temperature of the mixture at 0 °C. The reaction mixture was then stirred for an additional 15 minutes to ensure the reaction's completion.

B) Diazonium Coupling Reaction. [21]

A solution of 4- Chlorobenzaldehyde 2.8 g (0.02 mol) was prepared by dissolving it in 2.5 ml of a 10% NaOH solution. The resulting mixture was subsequently cooled to 0-5°C in an ice bath. Following the cooling step, the diazonium solution previously prepared, was added dropwise to the 4-Chlorobenzaldehyde solution. The mixture was continuously stirred and maintained at 0°C for one hour. Upon the formation of a precipitate and neutralization of the solution, the product was collected by filtration and washed with distilled water. The final compound was then recrystallized from ethanol. Table 1 displays the derivative (An1)'s physical characteristics.

Synthesis of Schiff bases (An2-An5) [22]

Cefdinir (1.58 g, 0.004 mol) was dissolved in 30 mL of ethanol with the addition of 8 drops of glacial acetic acid. Four parallel reactions were set up by adding one of the following compounds to separate solutions 4-bromobenzaldehyde (0.74 g, 0.004 mol), 4-methoxybenzaldehyde (0.54 g, 0.004 mol), acetophenone (0.48 g, 0.004 mol), and 4-bromoacetophenone (0.8 g, 0.004 mol). Following four hours of reflux heating and thirty minutes of cooling in an ice bath, the resulting particles were filtered out and recrystallized from ethanol. The physical properties of the derivatives of Schiff base derivatives (An2-An5) are shown in Table 1.

Table 1: Show some physical properties of compounds (An1-An5).

Compound No.	Molecular Formula	Molecular Weight(g/mol	Color	M.P °C	Yield %
An1	$C_{21}H_{15}ClN_6O_6S_2$	546.96	purple	225-227	82
An2	$C_{22}H_{19}N_5O_6\ S_2$	513.54	Yellow	231-233	72
An3	$C_{21}H_{16}BrN_5O_5S_2$	562.41	Brown	221-223	69
An4	$C_{22}H_{19}N_5O_5S_2$	497.54	Red	247-249	66
An5	$C_{22}H_{18}BrN_5O_5S_2$	576.44	White	252-254	71

Study of biological activity

In this study, four types of bacteria, positive and negative, were used, which are of great importance in the medical field due to their presence, including both types of *Staphylococcus aureus, enterococcus faecalis, klebsiella* and *Pseudomona*. The agricultural medium was also used as a Mueller-Hinton agar growth medium, in addition to microorganisms that were isolated from the laboratory of the College of Science, Biology Department, College of Science. After the results appeared, the biological activity of antibiotics and other pharmaceutical preparations was measured using Mueller-Hinton agar, which is also used to calculate the minimum inhibitory concentration (MIC). The compounds [An1, An2, An4] were dissolved and transferred to aqueous solutions at concentrations of 0.01, 0.001and 0.0001) mg/ml. Bacterial isolates were tested for susceptibility using DMSO [23, 24].

Results and Discussion

The synthesis of azo dye was achieved through the reaction of one mole of cefdinir with one mole of nitrous acid and 4-

chlorobenzaldehyde. Concurrently, Schiff bases were synthesized from the reaction of one mole of cefdinir with one mol either an aldehydes (such as 4-bromobenzaldehyde and 4-methoxybenzaldehyde) or ketones (such as acetophenone and 4-bromoacetophenone), as adepicted in Scheme 1.

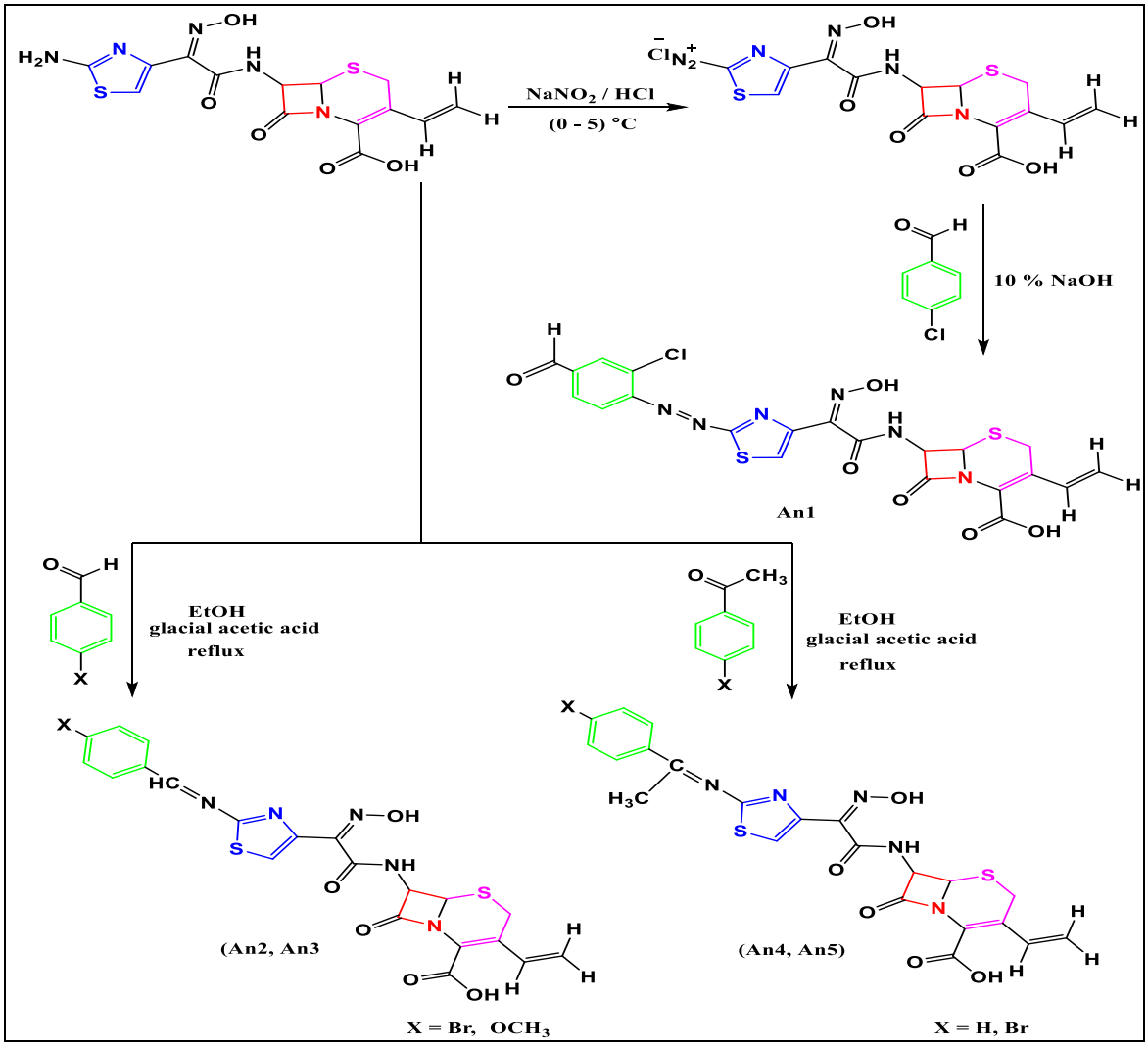

Scheme 1: Synthesis Pathway of compounds (An1-An5).

Interpreation of spectroscopy (FT-IR)

When analyzing the (FT-IR) spectrum of the azo dye compound (An1), as shown in Table 2 and Figures 2,the absorption bands of the amine group (NH_2) was completely absent, which indicates it was consumed during the reaction. Several functional groups were identified by the spectrum's distinctive absorption bands, which included an aromatic C-H stretch (υ(C-H)) at 3093 cm^{-1}, an alkyl C-H stretch at 2970 and 2877 cm^{-1}, and a hydroxyl group (υ(OH)) at 3304 cm^{-1}. It also displayed a C-N bond (υ(C-N)) at 1354 cm^{-1}, a lactam C=O stretch (υ(C=O)) at 1768 cm^{-1}, a carboxylic acid C=O stretch at 1683 cm^{-1}, and an N=N group (υ(N=N)) at 1624 cm^{-1} [25].

The full absence of the distinctive absorption band for the amine group (NH_2) in the FT-IR spectrum analysis of compound An2 (see Table 2 and Figure 3) verified the successful reaction. A lactam C=O stretch (υ(C=O)) at 1761 cm^{-1} [26], a carboxylic acid C=O stretch at 1728 cm^{-1}, an imine C=N stretch at 1651 cm^{-1}, a hydroxyl stretch (υ(OH)) at 3344 cm^{-1} [27], aromatic (3099 cm^{-1}) and aliphatic (2937 and 2899 cm^{-1}) C-H stretches, and a C-N bond stretch at 1354 cm^{-1} were also visible in the spectrum. As seen in Table 2 and Figure 4, compound An4's FT-IR spectra showed a number of distinctive absorption bands. Along with an aromatic C-H stretch at 3032 cm^{-1} and an aliphatic C-H stretch at 2970 cm^{-1}, a noticeable hydroxyl stretch (υ(OH)) was seen at 3348 cm^{-1}. Important carbonyl group stretches were also found, such as the carboxylic acid C=O at 1687 cm^{-1} and the lactam C=O at 1776 cm^{-1} [28]. The spectra also showed aromatic C=C bond vibrations at 1531 and 1516 cm^{-1}, as well as a C=N group stretch at 1616 cm^{-1}. Table 2 also displays the absorption statistics for further related substances.

Table 2: Characterization of absorption bands in FT-IR spectrum data in cm^{-1}

Compound No.	IR(KBr) υ . (cm^{-1})					
	υ (OH)	υ (C-H) Aromatic	υ (C=O) lactam	υ (C=O) carboxylic acid	υ (C=N) imine υ (N=N) azo	Other absorptions
An1	3304	3093	1768	1683	-1626	υ (C-Cl) 743 cm-1
An2	3344	3099	1761	1728	1651-	υ (C-O) 1045 cm-1
An3	3376	3077	1733	1698	1622 -	υ (C-Br) 745 cm-1
An4	3223	3032	1776	1687	1616 -	υ (C-H)aliphatic 2970, 2833cm^{-1}
An5	3348	3056	1746	1714	1634 -	υ (C-H)aliphatic 2967, 2825cm^{-1}

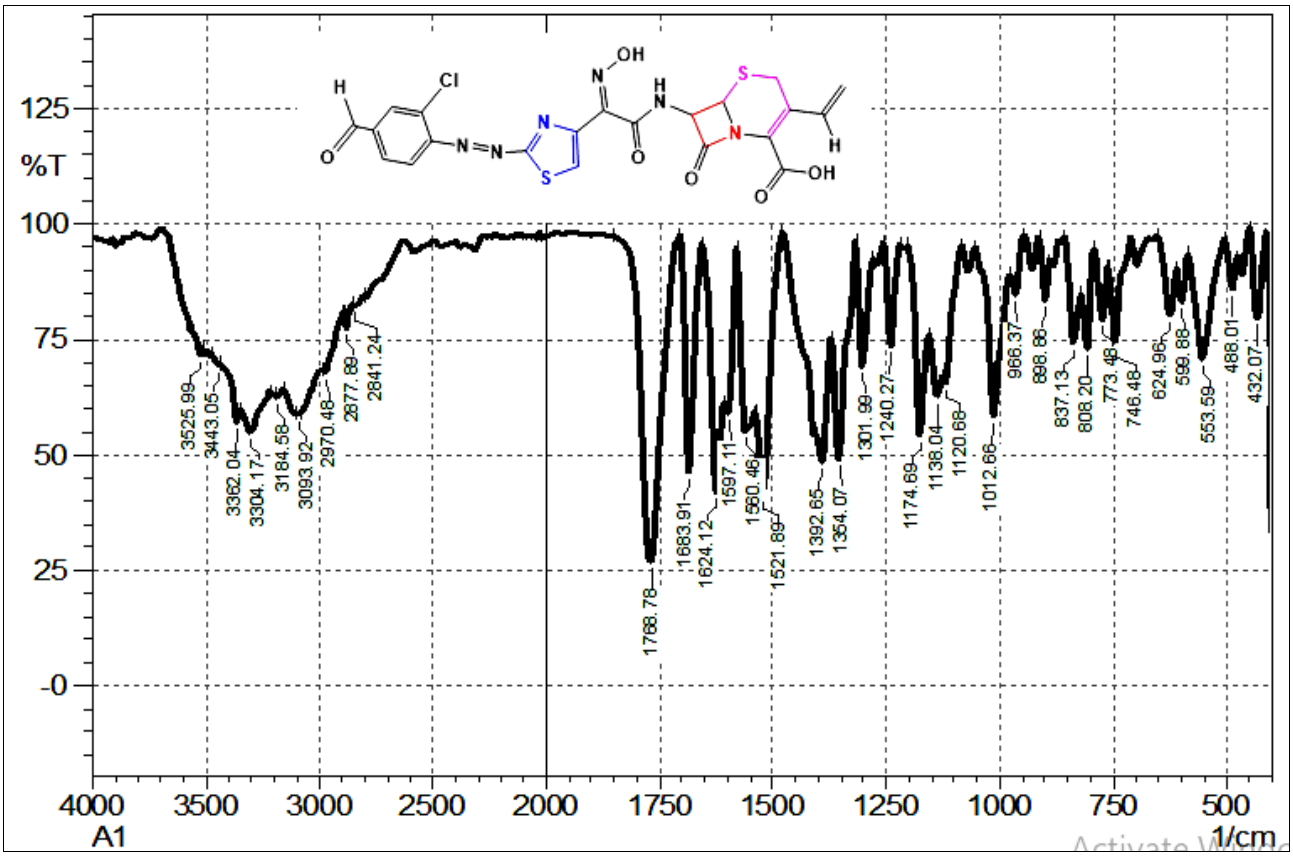

Fig 2: FTIR spectrum of derivative An1.

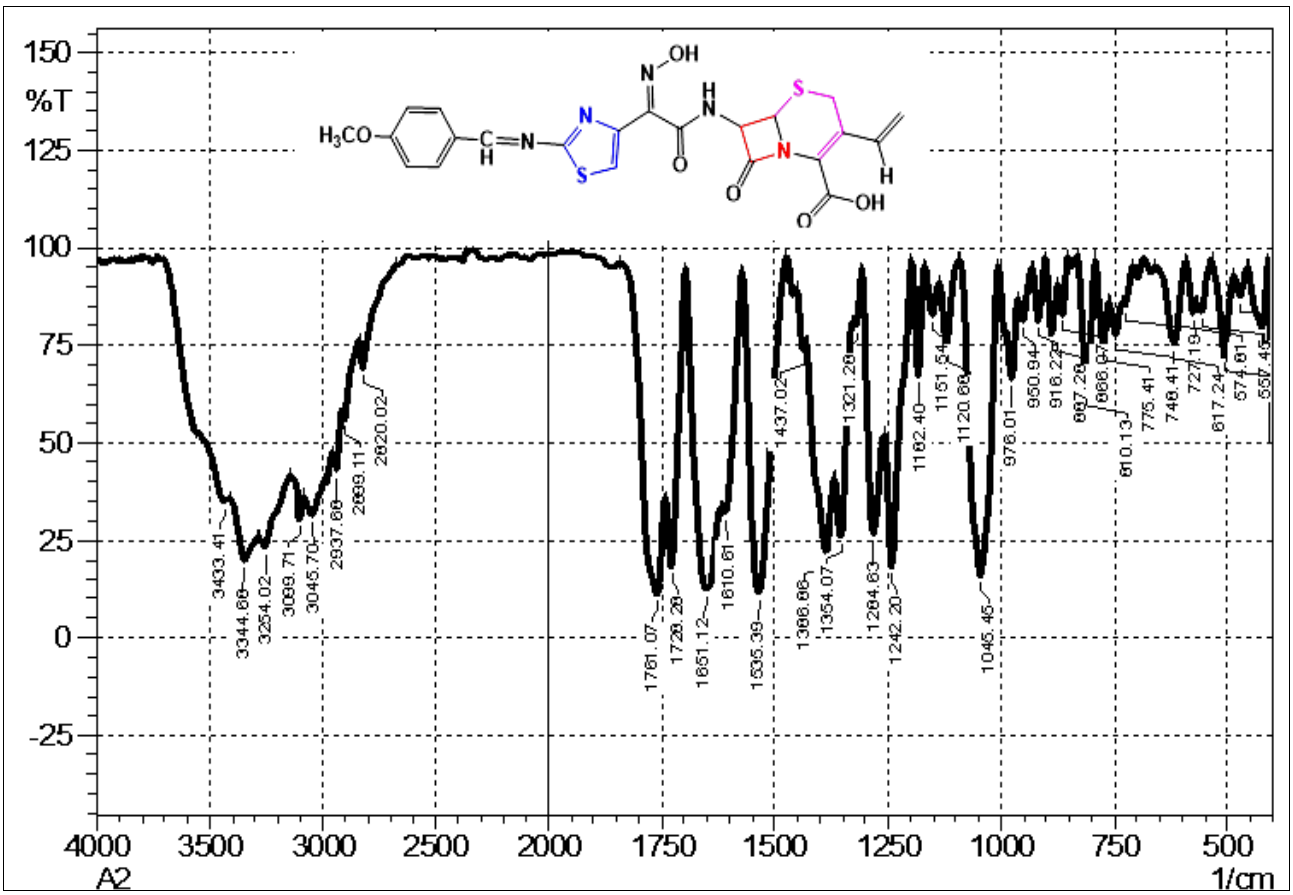

Fig 3: FTIR spectrum of derivative An2.

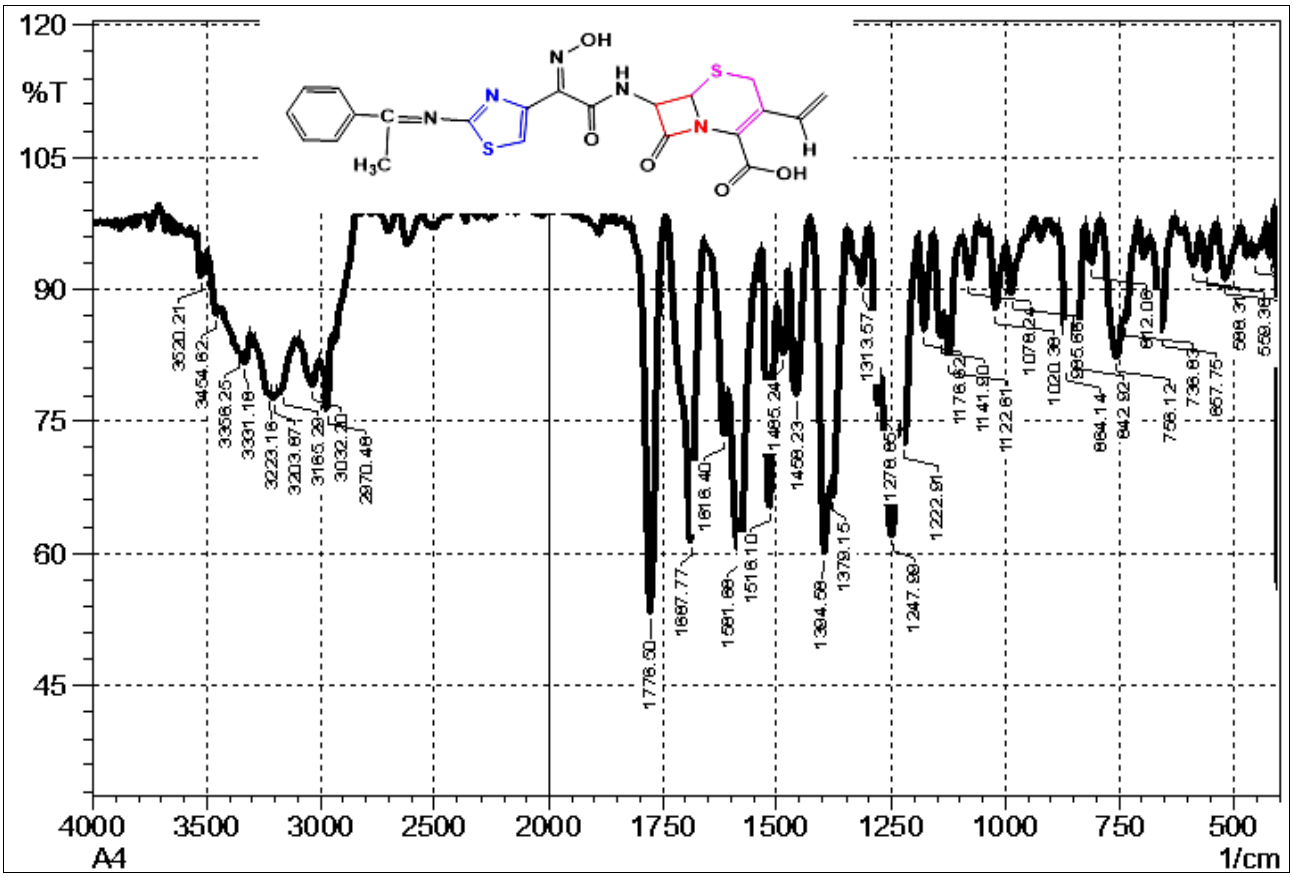

Fig 4: FTIR spectrum of derivative An4

Interpretation of spectroscopy (^{1}H-NMR, ^{13}C-NMR)

Compound An1 1H-NMR spectra (Figure 5) revealed a single signal for the proton on the methylene group next to sulfur (S-CH_2-) at (2.20) ppm (s, 2H). At 3.20 ppm (d, 1H), a doublet signal for the proton on the methine group (S-CH-) emerged. For the vinyl group (CH_2=CH-), two separate signals were detected: a triplet at (6.59) ppm (t, 1H) and a doublet at (5.95) (d, 1H) [29]. At (5.98) (d, 1H), a doublet representing the proton on the methine group next to the carbonyl and amine groups (CO-CH-NH) was seen. The multiplets at 7.21 and 7.49 ppm (m, 3H) were the aromatic protons (Ar-H). At 7.53 ppm (s, 1H), the proton on the thiazole ring (S=CH) was a singlet. At 7.51, 9.37, 9.81, and 13.39 ppm, respectively, the signals for the NH, COH, COOH, and N-OH protons were seen [30]. The 1H-NMR spectra of chemical An2 (Figure 6) revealed a single peak at (2.12 ppm)., which being assigend to the the methoxy group(-OCH_3) proton, A single signalat (2.34) ppm was given to the proton of the methylene group (S-CH_2-), placed next to sulfur. At (3.20) ppm, a doublet signal of the methine group (S-CH-CH-NH) proton was observed. The vinyl proton protons (CH_2=CH-) showed a doublet signal at (5.39) ppm. The CO-CH-NH group's methine proton was identified as the source of a doublet signal at 5.84 ppm. A multiplet between (7.20-7.39) ppm corresponded to the aromatic protons (Ar-H). The proton on the thiazole ring (S=CH) appeared as asingle signal at (7.51) ppm. The signals for the NH, CH=N, and N-OH protons apperred at 7.67, 7.82, and 7.84 ppm respectively. Compound An4 1H-NMR spectrum data (Figure 7) revealed a single signal at (1.22) ppm, which was identified as the (CH_3) proton [31]. A single signal at (2.45) ppm was observed for the methylene group protons adjacent to sulfur (S-CH_2-). A doublet signal appeared at (3.26) ppm for the methine group (S-CH-), while a doublet at (5.39) ppm was attributed to the (CH_2=CH-) proton, Another doublet was noted at (5.84) ppm and attributed to the (CO-CH-NH) proton [32]. The aromatic proton (Ar-H) showed a multiplet signal in the range of 7.20-7.51 ppm. A dditionally, a singlet for the thiazole ring proton(S=CH) was abserved at (7.67). Finally, the signals for the (NH), (-CH=N-), and (N-OH) protons appeared as signalest at 7.82, 7.84, and 9.56 ppm respectively.

The following signals were found in the 13C-NMR spectrum data for compound An1, which is shown in Figure 8. The (CH_2=CH) carbon is responsible for the signal at 23.35 ppm, whereas a (CH_2=CH) carbon is responsible for the signal at 109 ppm. It was determined that the aromatic (Ar-C) carbons were responsible for a multiplet signal in the 123-129 ppm region. The (N-CH=CH) carbon is responsible for the signal at (135) ppm. The (N-C=CH) carbon in the thiazole ring was identified as the source of a signal at (139) ppm. The (N-C=N) carbon in the same ring was identified as the source of a signal at (142) ppm. The (C=N-OH) carbon was identified as the source of a signal at (151) ppm. The (COOH) carbon was identified as the source of a signal at (164) ppm. The (CO-N) carbon was identified as the source of a signal at (169) ppm. Lastly, the (CO) carbon was identified as the source of a signal at (174) ppm. The 13C-NMR spectra of An4 shown in the figure 9 showed a signal at 23.3 ppm due to the S-CH_2 carbon atom, a signal at 114 ppm due to the N-C=C carbon atom, and a signal at 117 ppm due to the N-C=C carbon atom. As for the aromatic system carbon atoms, the spectrum showed multiple signals within the range of 125-135 ppm, and a signal at 151 ppm appeared due to the N-C=N-OH carbon atom, and a signal at 150 due to the carbon atom of the azetidine ring, and a signal at 154 ppm due to the carbon atom COOH, as a signal appeared at 156 ppm due to the carbon atom N-CO, and a signal at 158 ppm due to the carbon atom C=N, and at 164 ppm a signal appeared due to the carbon N-C=N.

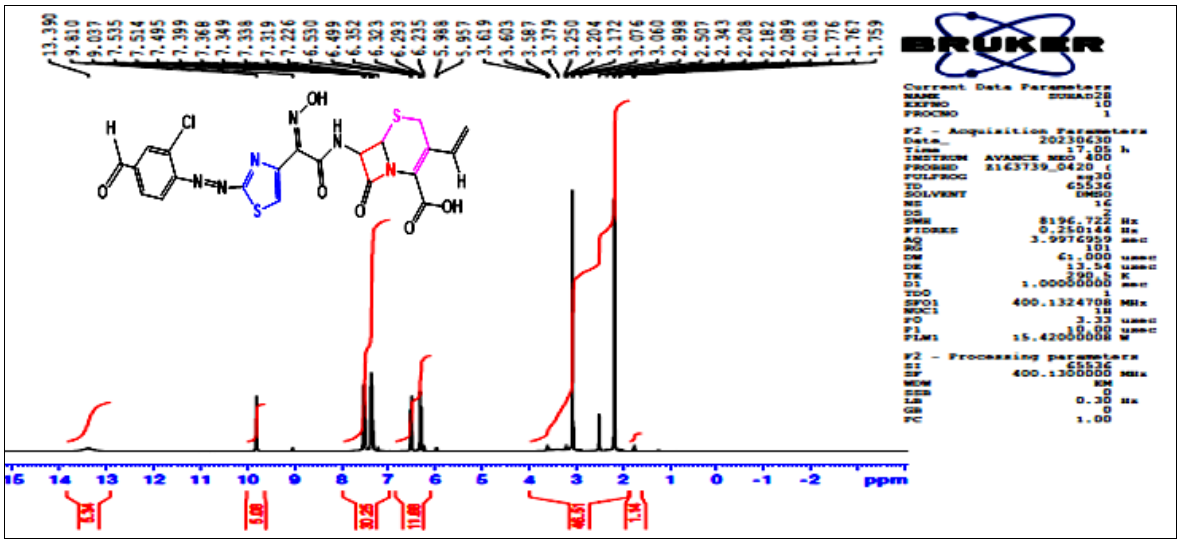

Fig 5: ^{1}H-NMR spectrum of derivative An1.

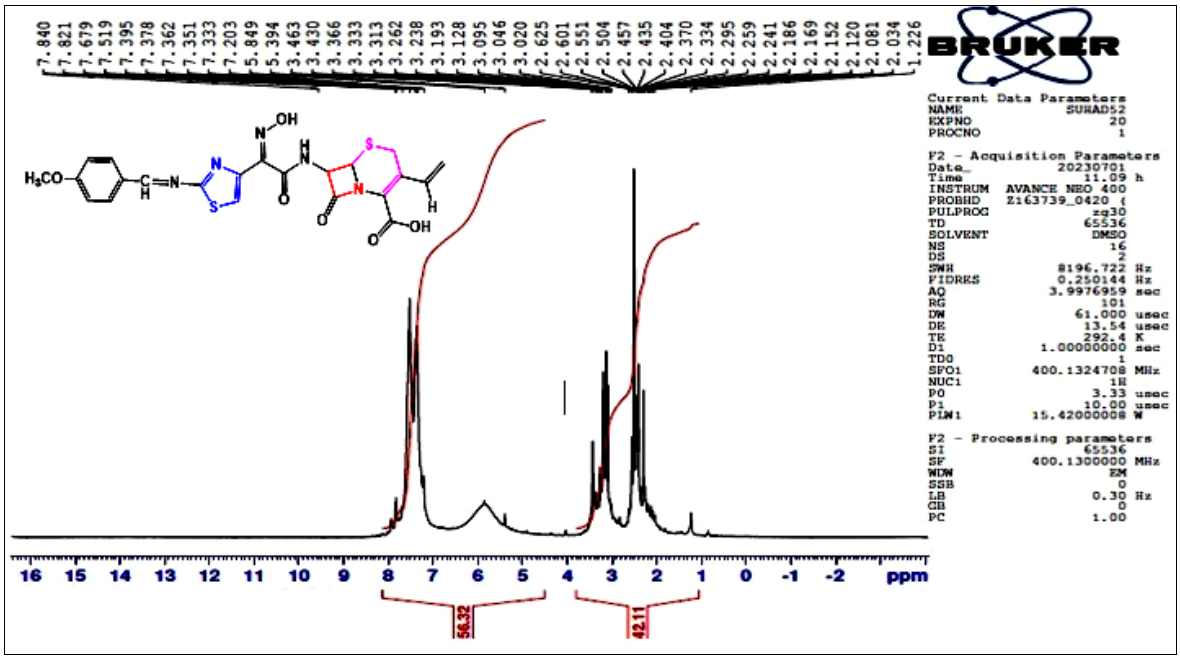

Fig 6: ^{1}H-NMR spectrum of derivative An2.

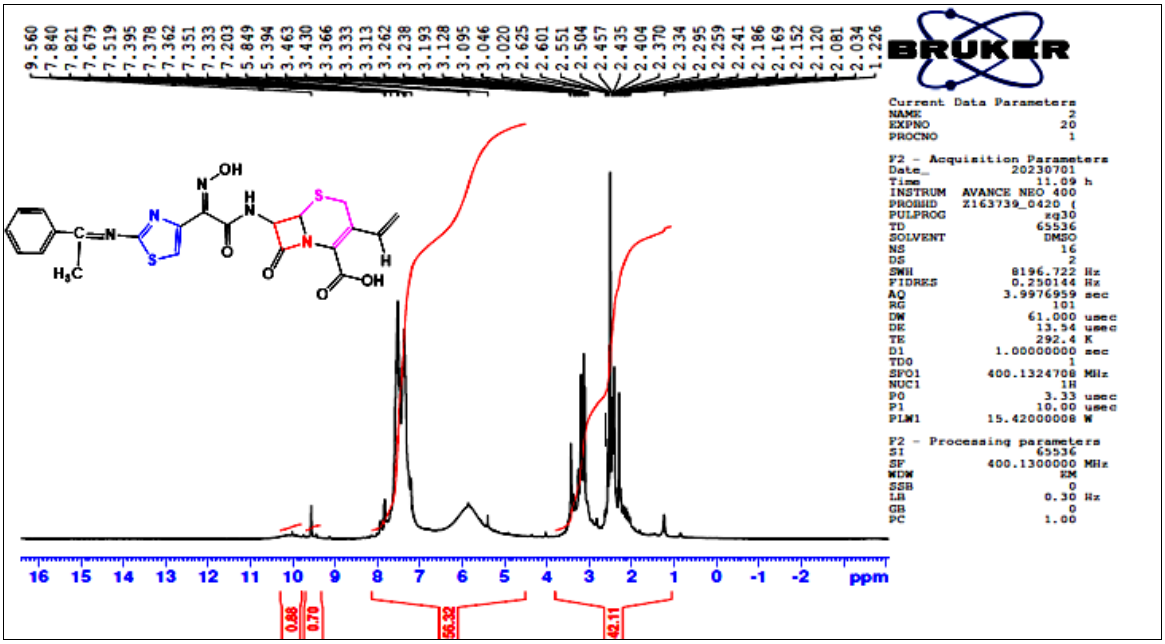

Fig 7: ^{1}H-NMR spectrum of derivative An4.

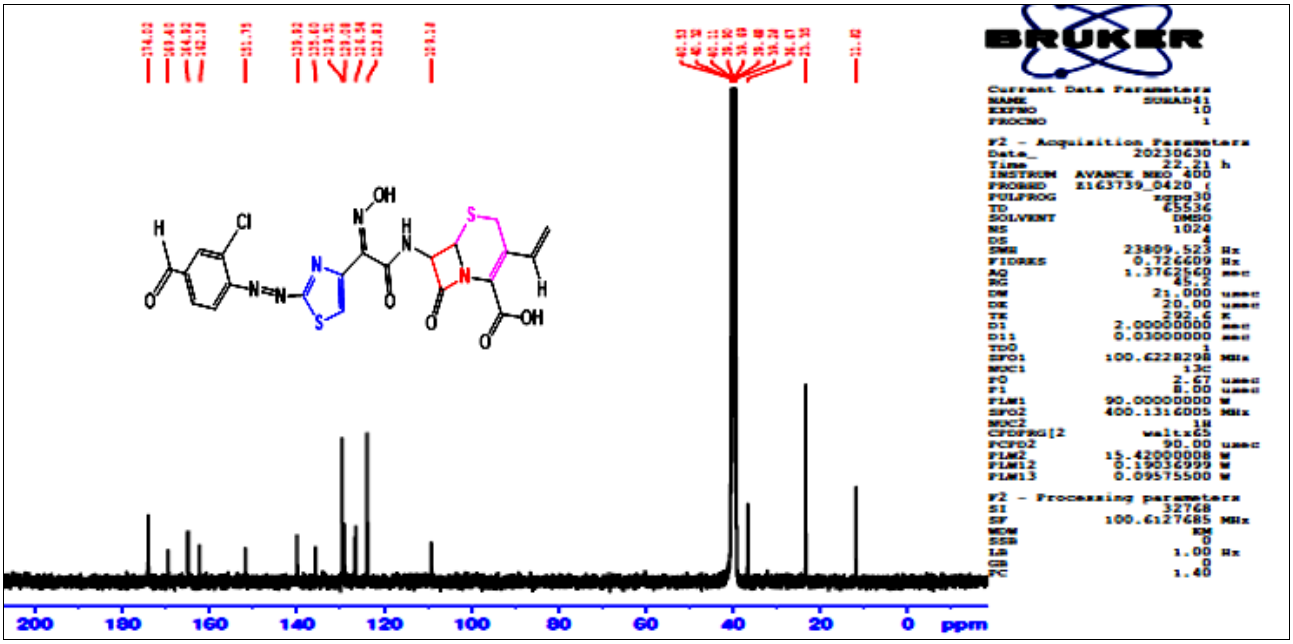

Fig 8: ^{13}C-NMR spectrum of derivative An1.

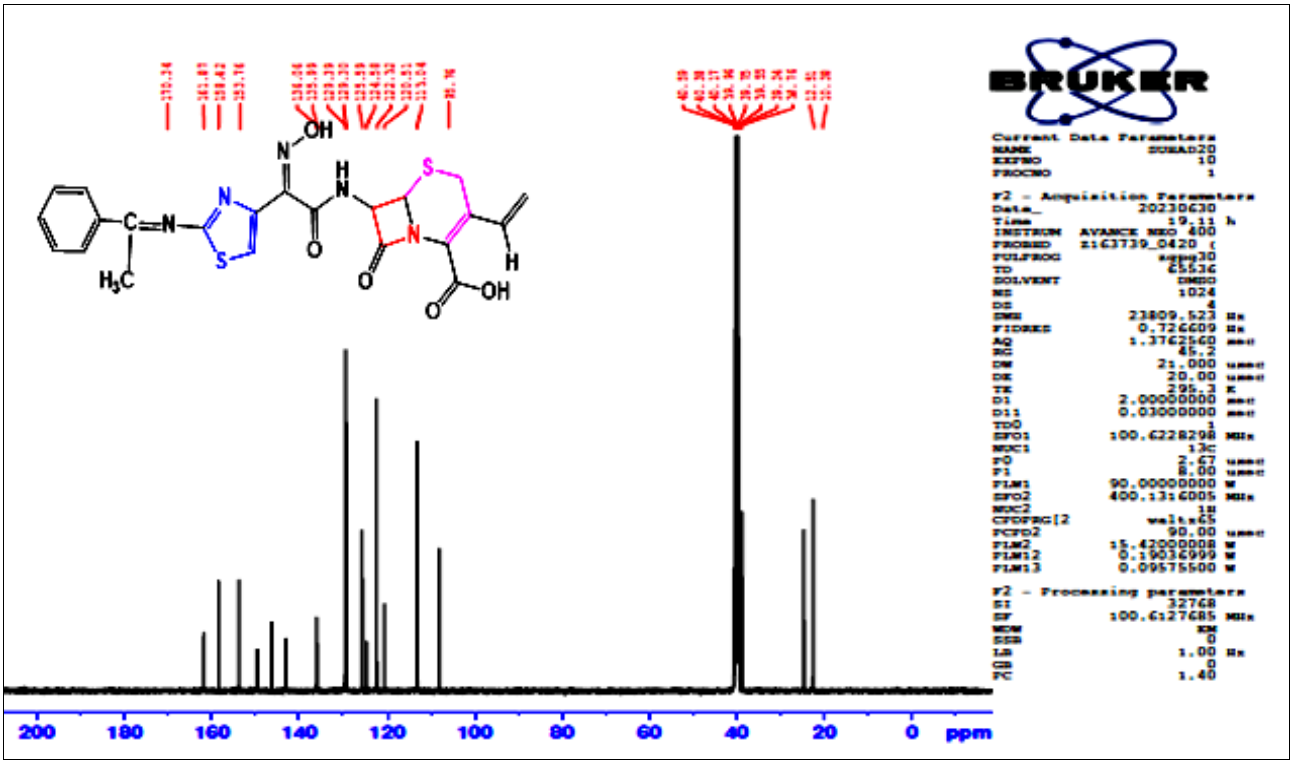

Fig 9: ^{13}C-NMR spectrum of derivative An4.

Interpretation of spectroscopy (Mass)

Mass spectrometry analysis of the prepared compounds An1 and An2 was performed to confirm their successful synthesis. Both compounds exhibited multiple molecular ionic peaks as shown in Table 3 and Figures 10 and 11. An1, which has a molecular mass of (546.96), is [$C_{21}H_{15}ClN_6O_6S_2$]. An ionic peak appeared at (m/q = 546) and the matching of the calculated molecular mass value of the compound with the molecular mass value of the ionic atom indicates the success of the preparation of the compound. A basic peak also appeared for the compound at m/q = 108)) [C_7H_8O]] +• This peak is the most abundant and indicates the presence of a stable formula for the compound during its ionization. This applies to the compound An2, which has a molecular mass of (531.54) [$C_{22}H_{19}N_5O_6S_2$] and which gave an ionic molecular peak at (513.4). The compound also had a baseline peak at m/q = 83.8 [C_5H_7O] +. This peak is the most abundant and indicates a stable form of the compound during ionization. The authenticity of the prepared compounds was confirmed by the baseline peak, while the remaining peaks that appeared in the mass spectrum confirmed the structural form of the compound.

Table 3: Mass spectrometric data for compounds An1 and An2.

Compound An1			Compound An2		
m/q	**Chemical Formula**	**Peak Type**	**m/q**	**Chemical Formula**	**Peak Type**
546.2	$[C_{21}H_{15}ClN_6O_6S_2]$	Molecular Ion Peak	513.4	$[C_{22}H_{19}N_5O_6S_2]$	Molecular Ion Peak
534.5	$[C_{20}H_{15}ClN_6O_6S_2]$+•	Fragment Peak	476.4	$[C_{19}H_{18}N_5O_6S_2]$+•	Fragment Ion
489.3	$[C_{19}H_{14}ClN_6O_4S_2]$+•	Fragment Peak	432.3	$[C_{18}H_{18}N5O_4S_2]$+•	Fragment Peak
466.5	$[C_{17}H_{15}ClN_6O_4S_2]$+•	Fragment Peak	418.3	$[C_{17}H_{16}N_5O_4S_2]$ +•	Fragment Peak
420.1	$[C_{16}H_{13}ClN_6O_4S]$ +•	Fragment Peak	394.3	$[C_{16}H_{18}N_4O_4S_2]$ +•	Fragment Peak
393.5	$[C_{15}H_{12}ClN_5O_4S]$ +•	Fragment Peak	351.1	$[C_{13}H_{10}ClN_5O_3S]$ +•	Fragment Peak
351.1	$[C_{13}H_{10}ClN_5O_3S]$ +•	Fragment Peak	321.1	$[C_{12}H_7ClN_4O_3S]$ +•	Fragment Peak
321.1	$[C_{12}H_7ClN_4O_3S]$ +•	Fragment Peak	378.3	$[C_{16}H_{18}N4O_3S_2]$	Fragment Peak
293.2	$[C_{11}H_7ClN_4O_2S]$	Fragment Peak	318.2	$[C_{14}H_{14}N_4O_3S]$	Fragment Peak
267.1	$[C_{11}H_{10}ClN_3OS]$	Fragment Peak	291.3	$[C_{13}H_{12}N_3O_3S]$ +•	Fragment Peak
240	$[C_9H_7ClN_3OS]$ +•	Fragment Peak	261.9	$[C_{12}H_{11}N_3O_2S]$ +•	Fragment Peak
182.9	$[C_8H_7ClN_2O]$ +•	Fragment Peak	244.9	$[C_{12}H_{10}N_3OS]$ +•	Fragment Peak
155.9	$[C_7H_6ClNO]$ +•	Fragment Peak	218.3	$[C_{11}H_{10}N_2OS]$ +•	Fragment Peak
141.0	$[C_7H_6ClO]$ +•	Fragment Peak	108.0	$C_7H_8O]$ +•	Fragment Peak
108.0	$[C_7H_8O]$ +•	**Base Peak**	205.2	$[C_{10}H_9N_2OS]$ +•	Fragment Peak
91.9	$[C_7H_7]$ +•	Fragment Peak	181.8	$[C_9H_{11}NOS]$ +•	Fragment Peak
			149.3	$[C_9H_{11}NO]$ +•	Fragment Peak
			107.9	$[C_7H_7O]$ +•	Fragment Peak
			83.8	$[C_5H_7O]$ +•	**Base Peak**
			57.9	$[C_3H_5O]$ +•	Fragment Peak

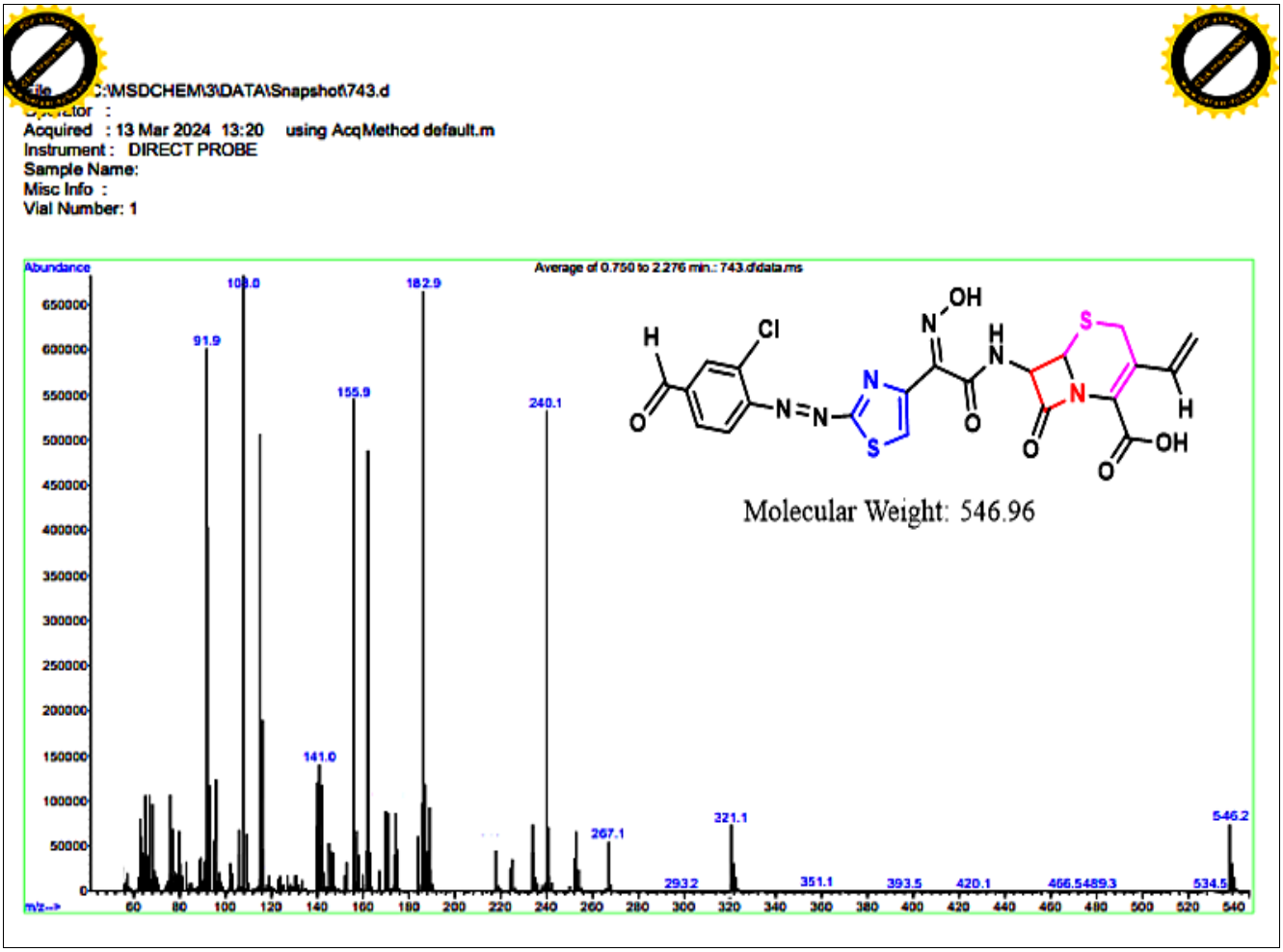

Fig 10: Mass spectrum (An1)

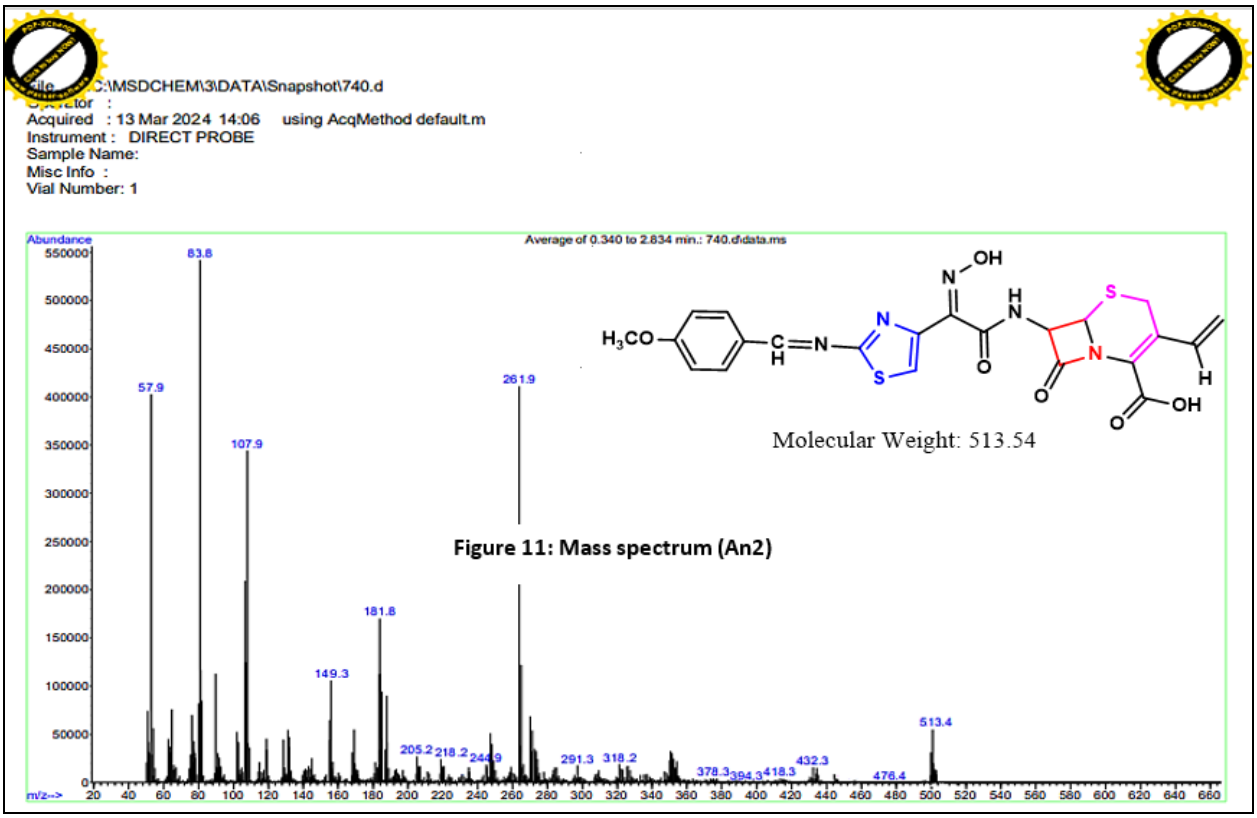

Fig 11: Mass spectrum (An2)

Analysis of the Scanning Electron Microscope (SEM)

Scanning electron microscopy is an effective analysis technique for microanalysis on a range of whole materials at large magnifications and for producing high-resolution images. The SEM technique is used to acquire pictures of material surfaces. The sample's various signals provide details on its exterior shape and crystalline structure, as well as whether or not it is a nanoscale material. Through it, a two-dimensional picture is produced that shows differences in characteristics. It can image typical regions with widths between 1 cm and 5 µm in scanning mode (possible resolution between 50 and 100 nm, magnification between 20X and about 30,000X). It can also evaluate the locations of specific points on the sample. These figure 12 illustrate the morphology and surface properties of the compounds, all imaged using a scanning electron microscope (SEM). Each image shows a different shape and size of the compound, reflecting variations in its preparation methods or crystalline properties. Figure 12 shows sharp needle-like nanostructures with micrometer dimensions, ranging in length from 1.2 to 1.8 micrometers. Figure 12(a), shows smaller, elliptical structures with dimensions ranging from 0.6 to 0.8 micrometers. Figure 12(b) shows spherical nanoparticles with diameters ranging from 390 to 480 nanometers. This variation in shape and size has a direct impact on the applications of each compound. Needled structures may be suitable for applications requiring a large surface area, such as catalysis or sensing, while spherical shapes may be desirable for applications such as drug delivery or nanocomposite manufacturing. These images provide crucial visual evidence of the success of various preparation processes and are used to assess the quality of the final product.

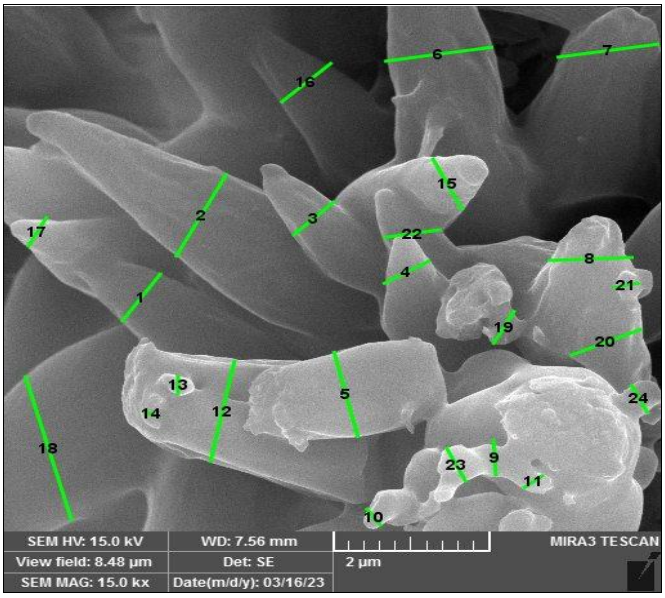

Fig 12 (a): SEM An1.

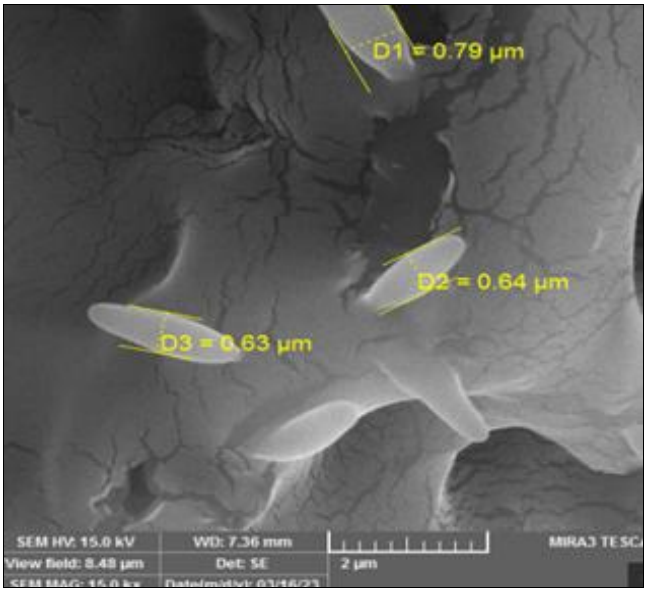

Fig 12 (b): SEM An*2*.

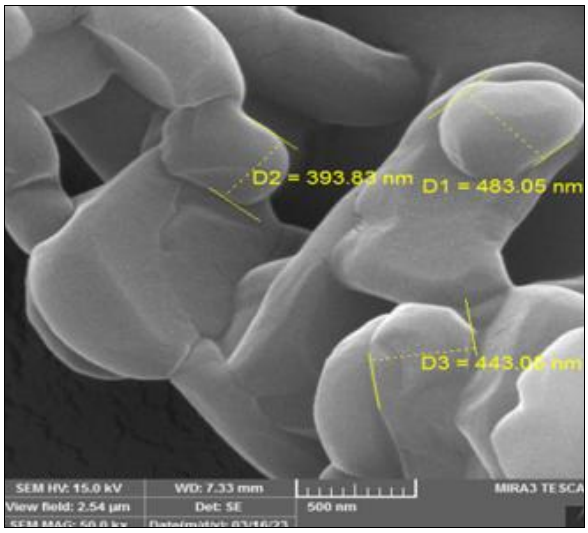

Fig 12 (c): SEM An*4*.

The Biological activity

The results show that the compounds have varying efficacy against different bacteria. Enterococcus faecalis is the most sensitive to these compounds, showing a large inhibition zone even at the lowest concentration. In contrast, Pseudomonas is the most resistant, with a sharp decline in efficacy as the compound concentration decreases. Klebsiella and Staphylococcus aureus exhibit intermediate sensitivity, with the compounds losing significantly in efficacy as their concentration decreases. Because gram-positive bacteria have different cell wall structures and contain virulence agents including capsules and biofilm agents, they are more resistant to the materials under study than gram-negative bacteria. These findings demonstrate that the type of bacteria and dosage utilized have a significant impact on the produced compounds' efficacy, as shown Figures 13, 14, and 15.

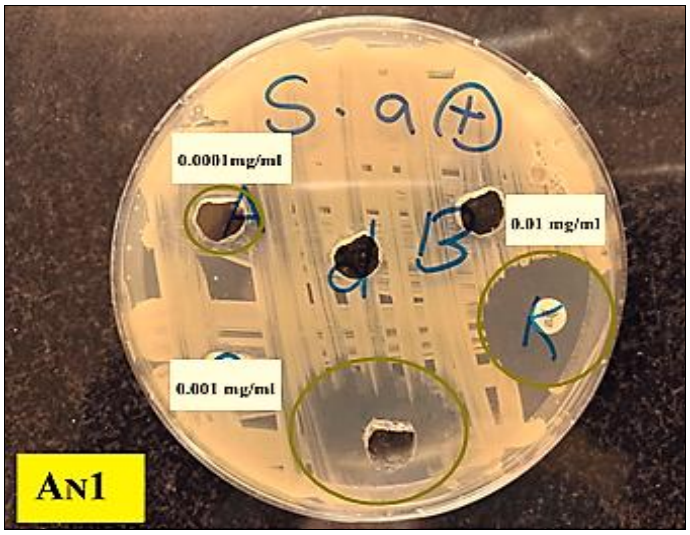

Fig 13 (a): Effect of Compound An1 on *Staph. aureus* Growth.

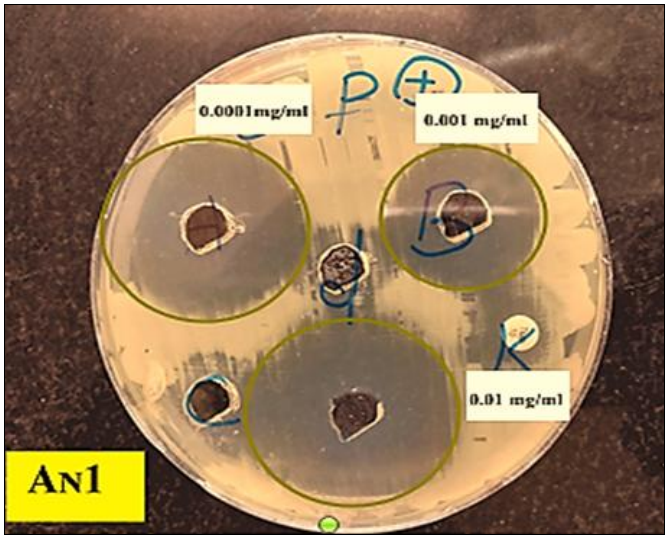

Fig 13 (b): Effect of Compound An1 on *E. faecalis* Growth.

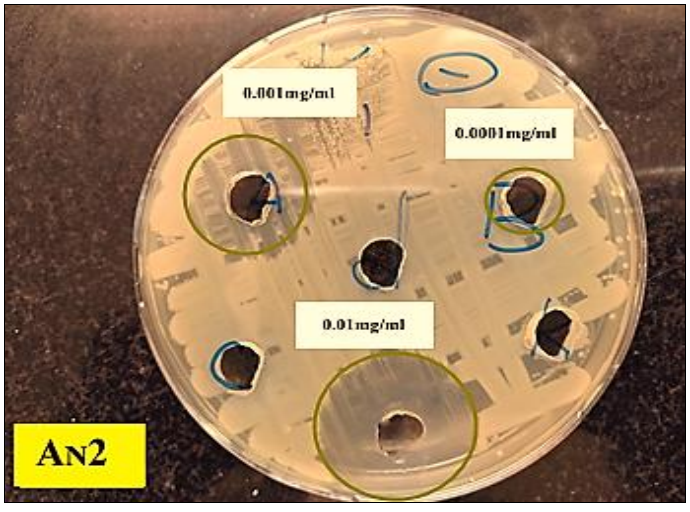

Fig 14 (a): Effect of Compound An2 on *Klebsiell*a Growth

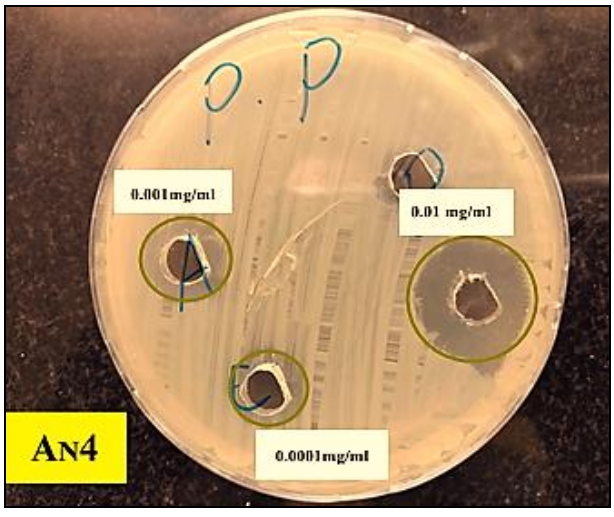

Fig 14 (b): Effect of Compound An4 on *Pseudomonas* Growth

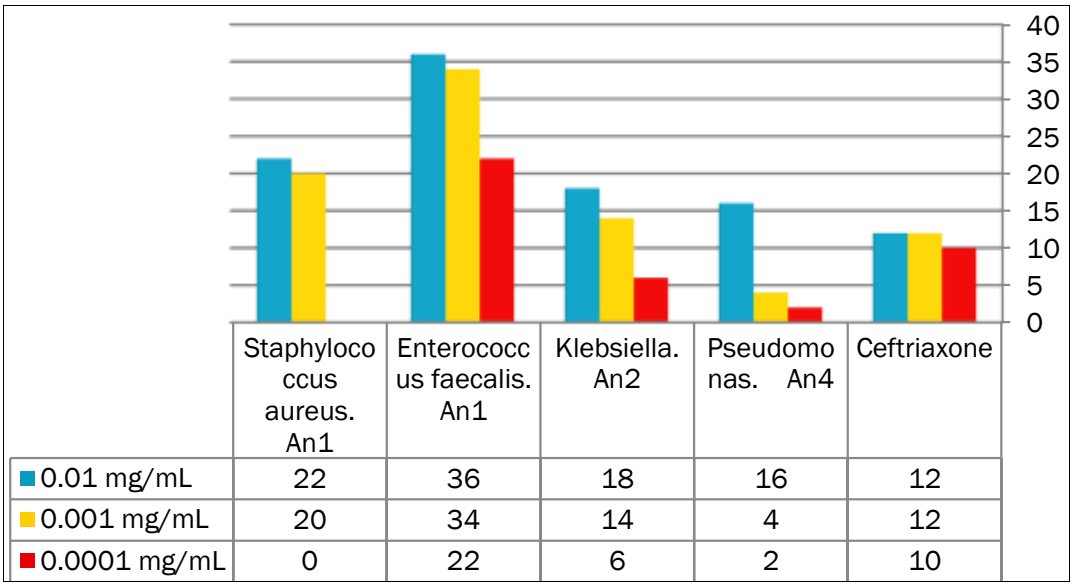

	Staphylococcus aureus. An1	Enterococcus faecalis. An1	Klebsiella. An2	Pseudomonas. An4	Ceftriaxone
0.01 mg/mL	22	36	18	16	12
0.001 mg/mL	20	34	14	4	12
0.0001 mg/mL	0	22	6	2	10

Fig 15: Biological activity of An1, An2, and An4 against bacterial strainst.

Molecular docking study

In addition to experimental techniques, AutoDock 4.2 was used to examine the interaction processes of An1, An2, and An4 as ligands with coagulase as targets. The crystal structure of coagulase (PDB ID: 2A1D) [34], was downloaded from proteindata bank The molecular electrostatic potential surface was analyzed to look into the reactive sites of the inhibitors under investigation's electrophilic and nucleophilic assaults. The adopted-basis Newton-Raphson technique and the reduced CHARMm force field were also used to prepare the selected target for molecular docking, and AutoDock 4.2 was used to complete the process [35].

Results

From the results of molecular docking in Table 3, it is clear that compounds An1, An2, and An4 have an equal binding energy of -8.5 kcal/mol, which is a good binding energy that supports the results of testing the compounds in culture media.

Table 3: binding energy, RMSD for An1, An2 and An4

compounds	Binding Energy	RMSD
An1	-8.5	0
An2	-8.5	0
An4	-8.5	0

The 2D and 3D shapes of the vehicles An1, An2 and An4 are shown in the following figures:

Figures 16 show the presence of hydrogen bonds, the first between the hydroxyl group attached to the imine in compound An1 with THR147 of the protein, the second between the lone pair of electron presence in the nitrogen atom of imine group with THR147 of the protein, and the third bond between the electron doublet on the nitrogen of the four-ring ring in compound An1 with THR150 of the protein. There is also a Pi-Sigma bond between the carbon of the alkene group of compound An1 with TRP50 of the protein, and three bonds between the double bonds in the five-membered ring of compound An1, the first in the form of Pi-Anion with GLU146 of the protein, and the other two in the form of Pi-Sulfur with both CYS201 and CYS231 of the protein.

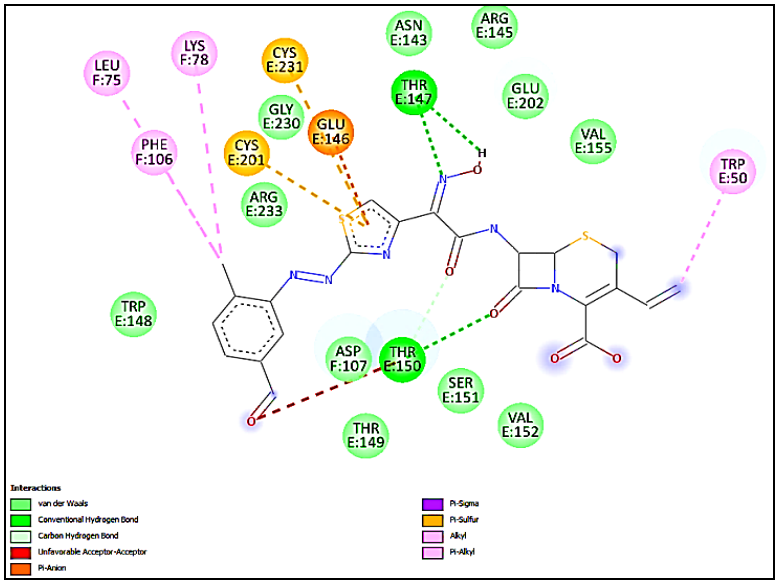

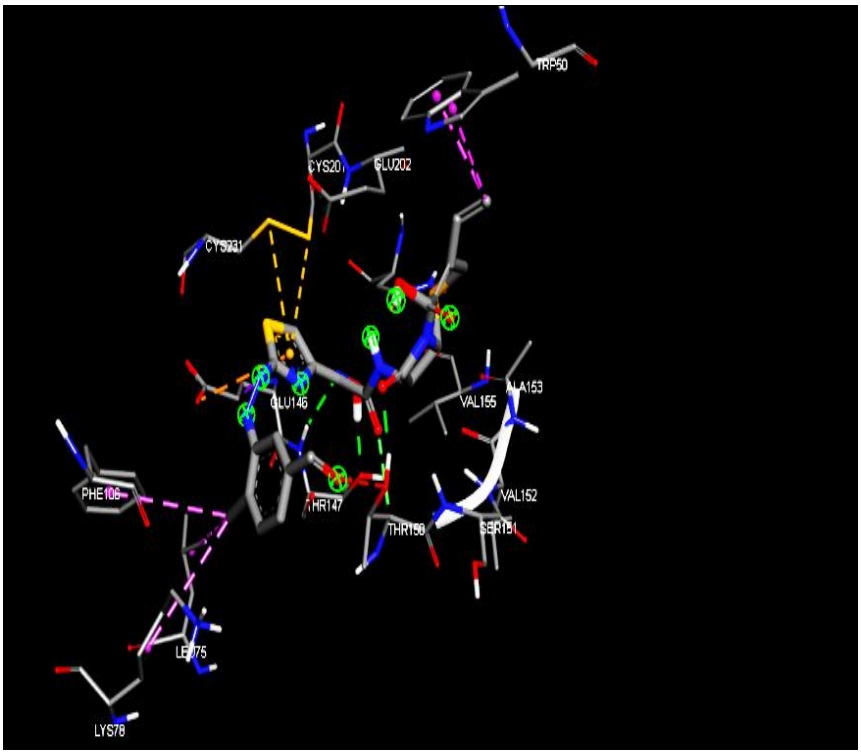

Fig 16: 2D, 3D imension model of An1 with coagulase.

Figures 17 demonstrate the presence of hydrogen bonds: the first is between the protein's ASN143 and the hydroxyl group attached to the imine in compound An2, the second is between the nitrogen atom of the imine group in compound An2 and THR147, the third is between the oxygen lone pair of the carbonyl group in compound An2 and THR150, and the final one is between the oxygen of the ether group of compound An2 and LYS78. Furthermore, a Pi-Sigma bond exists between the carbon of compound An1's alkene group and the protein's TRP50, and three bonds exist between the double bonds in compound An2's five-membered ring. The first bond is in the form of a Pi-Anion with the protein's GLU146, while the other two are in the form of a Pi-Sulfur with both CYS201 and CYS231 of the protein. Lastly, ASP107 of the protein and the carbon of the methyl group of chemical An2 form a carbon-hydrogen bond.

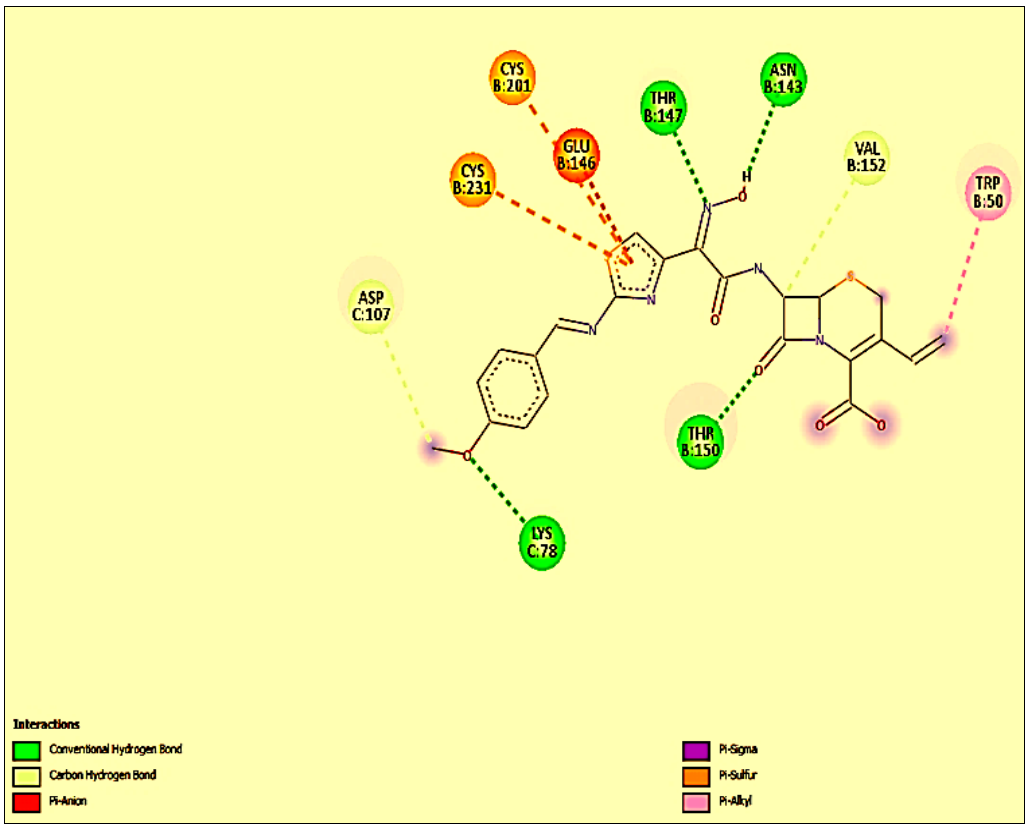

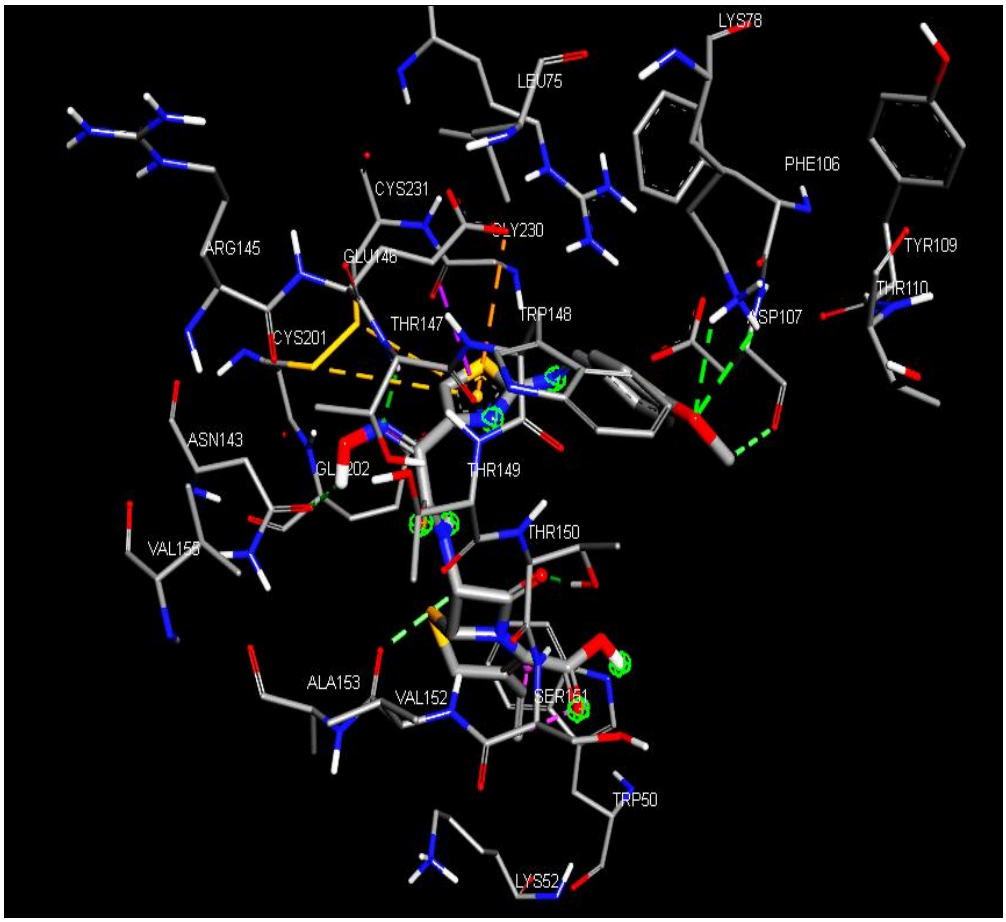

Fig 17: 2D, 3D imension model of An2 with coagulase.

Finally, figures 18 show the presence of three hydrogen bonds: the first between the hydroxyl group attached to the imine nitrogen of compound An4 and THR147 of the protein, the second and third between oxygen electron pair of the carbonyl group in compound An4 and THR150 and SER151 of the protein. In addition, there is a Pi-Sigma bond between the carbon of the alkene group of compound An4 with TRP50 of the protein and two bonds between the double bonds in the five-membered ring of compound A4, the first in the form of Pi-Anion with GLU146 of the protein, and the second in the form of Pi-Sulfur with CYS231 of the protein. Finally, there is a carbon-hydrogen bond between the carbon atom of the four-ring in compound An4 and VAL152 in the protein.

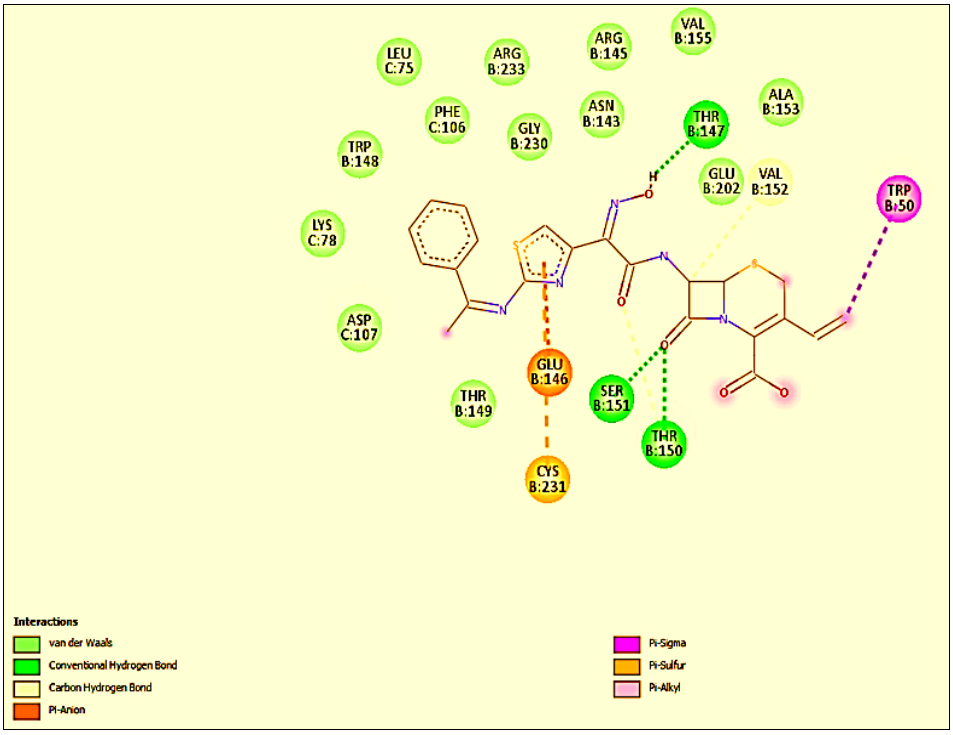

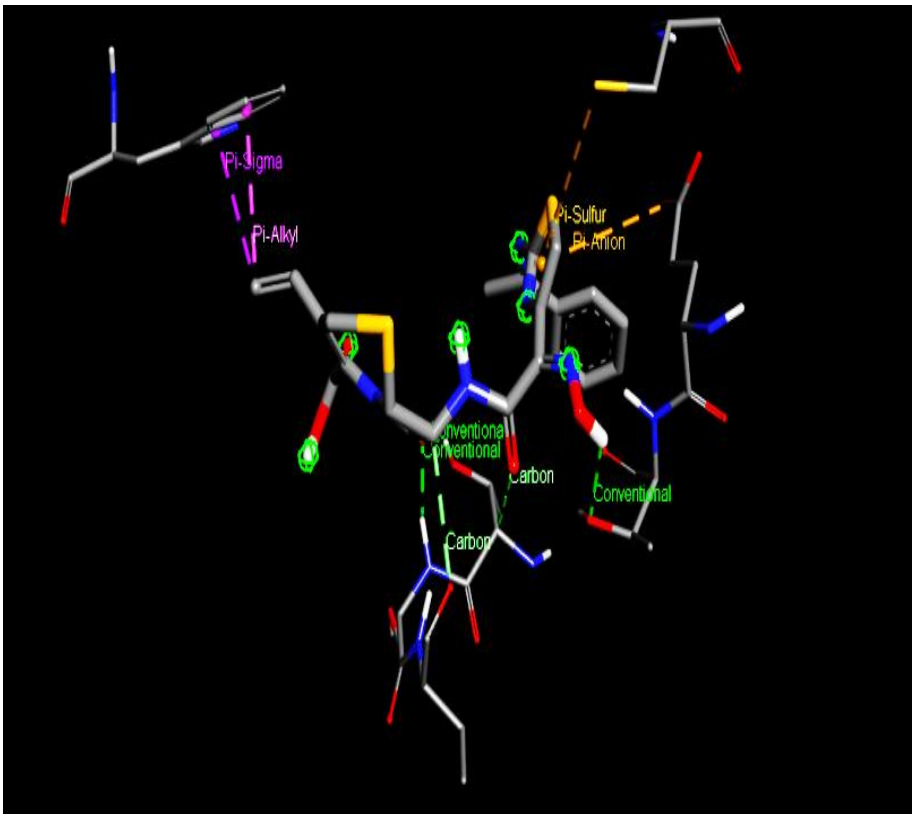

Fig 20: 2D, 3D imension model of An2 with coagulase.

Conclusions

In this research, new derivatives of cefdinir were prepared. The dye An1 was prepared by reacting cefdinir with sodium nitrite in the presence of concentrated hydrochloric acid to prepare the diazonium salt and then coupling the resulting diazonium salt with a benzaldehyde substitute in a basic medium in the presence of sodium hydroxide. Schiff base derivatives of cefdinir were also prepared by reacting cefdinir with benzaldehyde substitutes and acetophenone substitutes in the presence of glacial acetic acid and using ethanol as a solvent. The prepared compounds were characterized using spectroscopic methods, infrared spectra (FT-IR), 1H-NMR, and 13C-NMR spectra, in addition to using mass spectra to confirm the structural integrity of some of the prepared compounds. A mass spectrum analysis was performed for the compounds An1 and An2, and it was found that there is a match between the calculated molecular mass of the compounds and the measured molecular mass. This is evidence of the correctness of the structural integrity of the compounds and the success of the preparation process. The biological activity of compounds An1, An2, and An4 against two types of Gram-positive and Gram-negative bacteria was evaluated by the agar well diffusion method. It was found that these compounds have high activity against these types of bacteria, especially at high concentrations. Compound An1 showed inhibition zones of 36 mm and 22 mm against Enterococcus faecalis and Staphylococcus aureus, respectively, while compound An2 showed inhibition zones of 18 mm against Klebsiella pneumoniae, while An4 showed inhibition zones against Pseudomonas at high concentrations. At low concentrations, the compound showed inhibition zones of 34 mm and 22 mm against Enterococcus faecalis, while the remaining compounds were less effective at low concentrations. The molecular docking of AN1 and An4 with estrogen receptor alpha (PDB ID: 5T92) was studied and showed stable binding with an affinity of -8.43 Kcal/mol for An1 and -8.03 Kcal/mol for An4 compared to the standard compound at -7.92 Kcal/mol. Finally, the structures of compounds An1, An2, and An4 were analyzed using a scanning electron microscope, and it was found that these materials have different sizes and shapes, which indicates the difference in their crystalline properties and the difference in their preparation methods. This study confirms that the production of new compounds with multiple purposes can be achieved through structural control of these compounds and that future research can improve the effectiveness of these compounds in terms of their effectiveness in the body of the living organism.

Reference

1. Naama NA, Hameed GS, Hanna DB, Mahdi ZH. Formulation of cefdinir ternary solid dispersion and stability study under harsh conditions. Al Mustansiriyah Journal of Pharmaceutical Sciences. 2025;25(1):27-48.
2. Guay DR. Cefdinir: an advanced-generation, broad-spectrum oral cephalosporin. Clinical Therapeutics. 2002;24(4):473-489.
3. Mao N, Xu Z, Su J, Wang B, Xia J, Zheng D, *et al*. Bioequivalence of cefdinir dispersible tablets in healthy Chinese subjects under fasting and fed conditions: a single-centred, randomized, open, single-dose, two-preparation, two-cycle, two-sequence, double-crossover trial. Naunyn-Schmiedeberg's Archives of Pharmacology. 2025;398(6):6821-6829.
4. Gwaltney JM Jr, Savolainen S, Rivas P, Schenk P, Scheld WM, Sydnor A, *et al*. Comparative effectiveness and safety of cefdinir and amoxicillin-clavulanate in treatment of acute community-acquired bacterial sinusitis. *Cefdinir Sinusitis Study Group*. Antimicrobial Agents and Chemotherapy. 1997;41(7):1517-1520.
5. Selvi A, Salam JA, Das N. Biodegradation of cefdinir by a novel yeast strain, *Ustilago* sp. SMN03 isolated from pharmaceutical wastewater. World Journal of

Microbiology and Biotechnology. 2014;30(11):2839-2850.
6. Boltia S, Algmaal S, Mostafa N, El Saharty Y. Development and validation of a spectrofluorimetric method for the determination of cefdinir via its degradation products. Journal of Applied Spectroscopy. 2021;88(2):424-432.
7. Morina D, Sessevmez M, Sinani G, Mülazımoğlu L, Cevher E. Oral tablet formulations containing cyclodextrin complexes of poorly water-soluble cefdinir to enhance its bioavailability. Journal of Drug Delivery Science and Technology. 2020;57:101742.
8. Verma C, Quraishi M. Recent progresses in Schiff bases as aqueous phase corrosion inhibitors: design and applications. Coordination Chemistry Reviews. 2021;446:214105.
9. Raju SK, Settu A, Thiyagarajan A, Rama D, Sekar P, Kumar S. Biological applications of Schiff bases: an overview. GSC Biological and Pharmaceutical Sciences. 2022;21(3):203-215.
10. Mushtaq I, Ahmad M, Saleem M, Ahmed A. Pharmaceutical significance of Schiff bases: an overview. Future Journal of Pharmaceutical Sciences. 2024;10(1):16.
11. Al-Tufah MM. Synthesis and identification of some new bi-azetidine-2,2′-dione and bi-quinazoline-4,4′-dione compounds derived from bis-Schiff base derivatives. Samarra Journal of Pure and Applied Science. 2025;7(2):56-76.
12. Magalhães T, Da Silva C, Dos Santos L, Santos D, Silva L, Fuchs B, *et al*. Cinnamyl Schiff bases: synthesis, cytotoxic effects and antifungal activity of clinical interest. Letters in Applied Microbiology. 2020;71(5):490-497.
13. Hashem HE, Nath A, Kumer A. Synthesis, molecular docking, molecular dynamic, quantum calculation, and antibacterial activity of new Schiff base-metal complexes. Journal of Molecular Structure. 2022;1250:131915.
14. Meena K, Kumar Baroliya P. Synthesis, characterization, antimicrobial and antimalarial activities of azines-based Schiff bases and their Pd(II) complexes. Chemistry and Biodiversity. 2023;20(7):e202300158.
15. Rana MS, Rayhan NMA, Emon MSH, Islam MT, Rathry K, Hasan MM, *et al*. Antioxidant activity of Schiff base ligands using the DPPH scavenging assay: an updated review. RSC Advances. 2024;14(45):33094-33123.
16. Savcı A, Turan N, Buldurun K, Alkış ME, Alan Y. Schiff base containing fluorouracil and its M(II) complexes: synthesis, characterization, cytotoxic and antioxidant activities. Inorganic Chemistry Communications. 2022;143:109780.
17. Sandhu QUA, Pervaiz M, Majid A, Younas U, Saeed Z, Ashraf A, *et al*. Schiff base metal complexes as anti-inflammatory agents. Journal of Coordination Chemistry. 2023;76(9-10):1094-1118.
18. Sahu R, Shah K. Schiff bases: a captivating scaffold with potential anticonvulsant activity. Mini Reviews in Medicinal Chemistry. 2024;24(18):1632-1650.
19. Aljamali NM, Hassen HS. Review on azo-compounds and their applications. Journal of Catalyst and Catalysis. 2021;8(2):8-16.
20. Manjunatha B, Bodke YD, Nagaraja O, Nagaraju G, Sridhar M. Coumarin-benzothiazole-based azo dyes: synthesis, characterization, computational, photophysical and biological studies. Journal of Molecular Structure. 2021;1246:131170.
21. Maradiya HR, Patel VS. Synthesis and dyeing performance of some novel heterocyclic azo disperse dyes. Journal of the Brazilian Chemical Society. 2001;12(5):710-714.
22. Raouf OH, Selim S, Mohamed H, Abdel-Gawad OF, Elzanaty AM, Ahmed SAK. Synthesis, characterization and biological activity of Schiff bases based on chitosan and acetophenone derivatives. Asian Journal of Chemical Applications. 2020;3(4):274-282.
23. Al-Tufah M. Synthesis, identification, and biological activity of novel 1,3-oxazepane-7,4-dione compounds. Central Asian Journal of Theoretical and Applied Science. 2025;6(1):34-51.
24. Beebany S, Jasim SS, Al-Tufah MM, Arslan S. Preparation and identification of new 1,4-bis(5,3-substituted-2,3-dihydro-1H-pyrazole-1-yl)buta-1,4-dione derivatives with their antibacterial effect evaluation. Chemical Methodologies. 2023;7(2):123-136.
25. Yanai H, Hoshikawa S, Watanabe H, Kaneko H, Nakaminami H, Matsumoto T. Recyclable 2-fluoropyridine derivative as a storage for highly electrophilic 1,1-bis(triflyl)ethylene. Chemical and Pharmaceutical Bulletin. 2024;72(10):884-889.
26. Ellerbrock RH, Gerke HH. FTIR spectral band shifts explained by OM-cation interactions. Journal of Plant Nutrition and Soil Science. 2021;184(3):388-397.
27. Rao KP, Rani A, Reddy AR, Bharathi C, Dandala R, Naidu A. Isolation, structural elucidation and characterization of impurities in cefdinir. Journal of Pharmaceutical and Biomedical Analysis. 2007;43(4):1476-1482.
28. Madab DI, Al-Tufah MM. Synthesis and characterization of some new pyrazole and pyrimidine derivatives from chalcones and evaluation of their biological effectiveness. Central Asian Journal of Medical and Natural Science. 2025;6(3):1139-1154.
29. Patel S, Mandowara V, Gupta D, Parejiya P, Mehta D, Patel H, *et al*. Synthesis and physicochemical characterization of cefdinir prodrugs. 2016.
30. Jasm SS, Al-Tufah MM, Hattab AH. Synthesis, spectral characterization, and DFT analysis of novel 3-(4-substituted phenyl)-5-methyloxazolo[5,4-c]isoxazole derivatives. Asian Journal of Chemical Sciences. 2025;15(5):1-30.
31. Al-Tufah MM, Al-Badrany KA, Jasim SS. Synthesis and antibacterial evaluation of some new 1,5-benzoxazepine derivatives. Systematic Reviews in Pharmacy. 2021;12(3):270-285.
32. Ali AJ, Abbas MT, Hamdan IAA, Hamdan AAA, editors. Novel synthesis, characterization, antibacterial evolution and molecular modeling of Schiff base derived from R-camphor and five antibiotics from third generation of cephalosporin. IOP Conference Series: Materials Science and Engineering. 2019; IOP Publishing.
33. Montaser AS, Wassel AR, Al-Shaye'a ON. Synthesis, characterization and antimicrobial activity of Schiff bases from chitosan and salicylaldehyde/TiO_2 nanocomposite membrane. International Journal of Biological Macromolecules. 2019;124:802-809.
34. Kakkassery JT, *et al*. *In vitro* antibacterial and in silico docking studies of two Schiff bases on *Staphylococcus aureus* and its target proteins. Future Journal of Pharmaceutical Sciences. 2021;7(1):1-9.
35. Fawzi M, *et al*. A novel D-limonene derivative: synthesis, characterization, molecular docking, molecular dynamics and ADMET prediction studies. Journal of Sulfur Chemistry. 2024;45(6):831-849.